Applications of magnetic resonance elastography to healthy and pathologic skeletal muscle.

S.I. Ringleb, S.F. Bensamoun, Q. Chen, Armando Manduca, R.L. Ehman, Kai-Nan An

Invited Review

Applications of Magnetic Resonance Elastography to Healthy and Pathologic Skeletal Muscle

Stacie I. Ringleb, PhD,[1] Sabine F. Bensamoun, PhD,[1] Qingshan Chen, MS,[1] Armando Manduca, PhD,[2] Kai-Nan An, PhD,[1] and Richard L. Ehman, MD[2]*

Magnetic resonance elastography (MRE) is capable of noninvasively quantifying the mechanical properties of skeletal muscles in vivo. This information can be clinically useful to understand the effects of pathologies on the mechanical properties of muscle and to quantify the effects of treatment. Advances in inversion algorithms quantify muscle anisotropy in two-dimensional (2D) and three-dimensional (3D) imaging. Databases of the shear stiffness of skeletal muscle have been presented in the relaxed and contracted states in the upper extremity (biceps brachii, flexor digitorum profundus, and upper trapezius), distal leg muscles (tibialis anterior, medial gastrocnemius, lateral gastrocnemius, and trapezius), and proximal leg muscles (vastus lateralis, vastus medialis, and sartorius). MRE measurements have successfully validated a mathematical model of skeletal muscle behavior in the biceps brachii, correlated to electromyographic data in the distal leg muscles and quantified the effects of pathologies on the distal and proximal leg muscles. Future research efforts should be directed toward improving one-dimensional (1D) and 3D MRE data acquisition and image processing, tracking the effects of treatment on pathologic muscle and correlating the shear stiffness with clinical measurements.

Key Words: magnetic resonance elastography; skeletal muscle; elastic properties; biomechanics; shear stiffness
J. Magn. Reson. Imaging 2007;25:301–309.

WHEN THE FUNCTION of skeletal muscle is altered due to pathology or injury, it is difficult to objectively measure these changes. Most injuries to muscle are clinically assessed with functional examinations (e.g., the manual muscle test), validated clinical scales (e.g., modified Ashworth scale), force measurements using handheld and isokinetic dynamometers, and surface and fine wire electromyography (EMG). While these measurements provide information that clinicians can use to track the changes in muscle function in their patients, some are subjective or unreliable. Other methods such as the isokinetic dynamometer measure external torque, which can quantify how pathology affects a group of muscles, but it cannot provide information about the physiologic behavior of muscles or quantify the mechanical properties of individual muscles. Surface EMG can only record the activity of muscles that are close to the surface of the skin, fine wire EMG can be painful, and both methods only measure the activity of a small portion of the muscle. Instead of measuring functional changes, quantifying the elastic properties of skeletal muscle may help improve our understanding of the underlying causes of functional changes. Additionally, when the elastic properties are assessed under load and/or under various joint positions, both the muscle function and elastic properties can be measured simultaneously.

Toward the goal of measuring elastic properties of muscle, handheld devices have been developed that purport to assess in vivo muscle stiffness (1–3). These devices function by monitoring the resistance of soft tissue to a load imposed perpendicular to the tissue. Although they have acceptable reliability (1,4), they can only examine superficial muscles with parallel fiber orientations that are easily accessible with their transducer (1) and cannot simultaneously examine portions of a muscle with pennate or bipennate fiber orientations, such as the vastus medialis. The devices are also unable to differentiate between muscle and other subcutaneous tissues or changes in soft tissue tension transmitted to the region under the sensor via fascia from muscles that are remote from the sensor.

Recently, imaging techniques have been applied to investigate muscle function. Spin-tagging and phase-contrast MRI techniques can examine tissue velocity and how it changes when injury and pathology are present (5–8). Cine displacement encoding with stimulated echoes (DENSE) MRI can measure the displacements and strains in skeletal muscle during joint motion (9). T_2 mapping of muscle can be used to assess the effects of exercise intensity on the muscles (10–12). Muscle spectroscopy has been used to investigate lipid

[1]Biomechanics Laboratory, Division of Orthopedic Research, Mayo Clinic, College of Medicine, Rochester, Minnesota, USA.
[2]Department of Radiology, Mayo Clinic College of Medicine, Rochester, Minnesota, USA.
Contract grant sponsor: National Institutes of Health (NIH); Contract grant numbers: EB00812, EB01981, CA91959, HD07447.
*Address reprint requests to: R.L.E., M.D., Department of Radiology, Mayo Clinic College of Medicine, 200 First Street SW, Rochester, MN 55905. E-mail: ehman.richard@mayo.edu
Received March 21, 2006; Accepted September 15, 2006.
DOI 10.1002/jmri.20817
Published online in Wiley InterScience (www.interscience.wiley.com).

metabolism, diseased tissue, and muscle energetics in a research setting (13). Blood oxygenation level dependent (BOLD) imaging is being investigated as a method to measure microvascular density and/or reactivity in contracting skeletal muscle (14). While these methods provide useful information about in vivo muscle, they are unable to provide information about the material properties of muscle in situ.

Sonoelastography, a technique using ultrasound to measure the propagation of shear waves induced by vibrations applied at various frequencies, was used to estimate the elastic modulus of relaxed and contracted quadriceps muscle group (15). Subsequently, transient elastography was applied to muscle to quantify the anisotropic properties of muscle tissue (16–18). While both ultrasound elastography techniques are capable of estimating Young's modulus of muscle, ultrasound has a limited field of view. Additionally, the higher frequencies required for this technique can be rapidly absorbed by the muscle and may not penetrate into deeper muscles (19). Furthermore, it may be difficult to assess the mechanical properties of muscle when there is a complex bone-muscle geometry (19), it is not possible to obtain 3D data and it may be difficult to consistently scan the same area within a muscle.

Despite the advances in clinical evaluations and imaging techniques, there remains a need for methodology to noninvasively quantify the mechanical properties of skeletal muscle for evaluation of clinical cases and is also capable of examining the mechanical properties of muscle in three dimensions. Magnetic resonance elastography (MRE) is a noninvasive phase-contrast MR technique that uses an acoustic or mechanical driver to induce shear waves into the object of interest (20,21). An oscillating motion-sensitizing gradient synchronized to the mechanical vibration induces a measurable phase shift, which directly images the induced shear waves and allows us to calculate displacement at each voxel. These data can be inverted to estimate the shear modulus in any soft tissue. By estimating the shear stiffness of muscle using MRE, the underlying cause of functional changes can be quantified in vivo. Conversely, the aforementioned clinical assessments and imaging techniques assess the affects of the changes in the properties of the muscle. Additionally, MRE can directly quantify the passive and active properties of a muscle and can image muscle groups on both sides of a joint in one acquisition, which can allow us to investigate events such as cocontractions that affect the properties of multiple muscles simultaneously.

Knowing the mechanical properties of skeletal muscle has applications in several fields, including orthopedics, sports medicine, physical medicine and rehabilitation, endocrinology, and rheumatology. In orthopedics and sports medicine, MRE can be used to evaluate the effects of injury and track treatment methods to ensure that the correct muscles are being rehabilitated and to the correct degree. Using MRE to investigate the effects of treatment for patients with muscle spasticity (e.g., stroke, spinal cord injury, cerebral palsy, and brain injury) will allow us to objectively quantify the effects of an intervention instead of using subjective or qualitative measurements. With the potential for greater sensitivity with MRE than current techniques to detect change, beneficial medication or rehabilitation interventions could be more rapidly incorporated into clinical practice. If MRE measurements can be correlated with muscle biopsy, MRE could prove advantageous as a technique to detect diseases such as myositis, which currently can only be diagnosed with a biopsy. Finally, measurements of the properties of muscle may shed light on the effects of pathologies that change muscle fiber composition, like hyperthyroidism, and help improve our approach for treating individuals affected by these disorders.

Current MRE research efforts include implementing new pulse sequences to reduce scan time and investigate the behavior of shear waves in three dimensions, imaging the change in muscle tension as the level of contraction changes, and studying the anisotropy of muscle tissue. These efforts will lead to a more complete understanding of muscle tissue and when implemented to study pathologic conditions, our understanding of the effects of pathologies on muscle will be improved.

MRE DATA ACQUISITION

MRE can be implemented in a standard 1.5T or 3T whole-body scanner, in which a motion-sensitizing gradient is superimposed and switched in polarity at the frequency of the induced shear waves. While most systems are capable of inducing and measuring shear waves from 75 to 500 Hz, frequencies of 90 to 150 Hz are typically used in skeletal muscle. Shear waves have been induced with electromechanical (19,22–26), piezoelectric (27), electromagnetic coil (28), a piezoelectric bending element attached to a standard acupuncture needle (29), and pneumatic drivers (30). The induced cyclic motion has a wave vector, $\vec{k}$ at a given frequency (1/T). In the presence of motion-sensitizing gradients the cyclic motion causes a measurable phase shift in the in the received MR signal, given in Eq. [1] (20,21).

$$\phi(\vec{r},\theta) = \frac{\gamma N T(\vec{G}_0 \cdot \vec{\xi}_0)}{2} \cos(\vec{k} \cdot \vec{r} + \theta). \qquad (1)$$

The accumulated phase shift, φ, is proportional to the number of gradient cycles (N), the period of the gradient waveform (T), the displacemetn amplitude vector ($\vec{\xi}$), the motion-sensitizing magnetic gradient vector ($\vec{G}_0$), and the relative phase of the mechanical and magnetic oscillations (θ). The spin position vector is $\vec{r}$ and the gyromagnetic ratio is γ.

Typical data acquisition parameters for 2D acquisitions are as follows: TR = 100–350 msec, TE is defined as the minimum time required for motion encoding (10–60 msec), acquisition matrix size = 256, and a flip angle from 10° to 60°. Four or eight phase offsets are typically acquired and one to three 2D slices are acquired per acquisition. Each acquisition measures one component of motion, in the direction of the motion sensitizing gradient. To obtain all three components of displacement, the experiment must be performed three times with orthogonal motion sensitizing gradient directions. Depending on the number of offsets and slices

acquired, acquisition time typically ranges from 30 to 300 seconds.

Because the mechanical properties of muscle are affected by joint position and loading, positioning and loading devices have been developed to acquire muscle data. To test the biceps under load, a pulley system consisting of a hand grip at one end and weights at the other end was used (23). The muscles in the lower limb were tested in a relaxed configuration with the volunteer lying prone (27). These muscles were also tested under loads in three devices: 1) a positioning and loading device capable of adjusting the position of the ankle joint where weights connected to a cable and pulley system applied plantar flexion and dorsiflexion moments (Fig. 1a), thus investigating an isotonic contraction (19,22,24); 2) a foot plate with a strain gauge incorporated to measure isometric force with the ankle fixed in neutral (31); and 3) using a positioning and loading device with a MR compatible torque cell to measure isometric moments and allowing for passive joint positioning (Fig. 1b) (26,32). A leg press containing MR-compatible load cells (Fig. 1c) (30), as well as a loading and positioning device consisting of a cable and pulley system to load the leg while fully extended (25), was used to assess the thigh muscles.

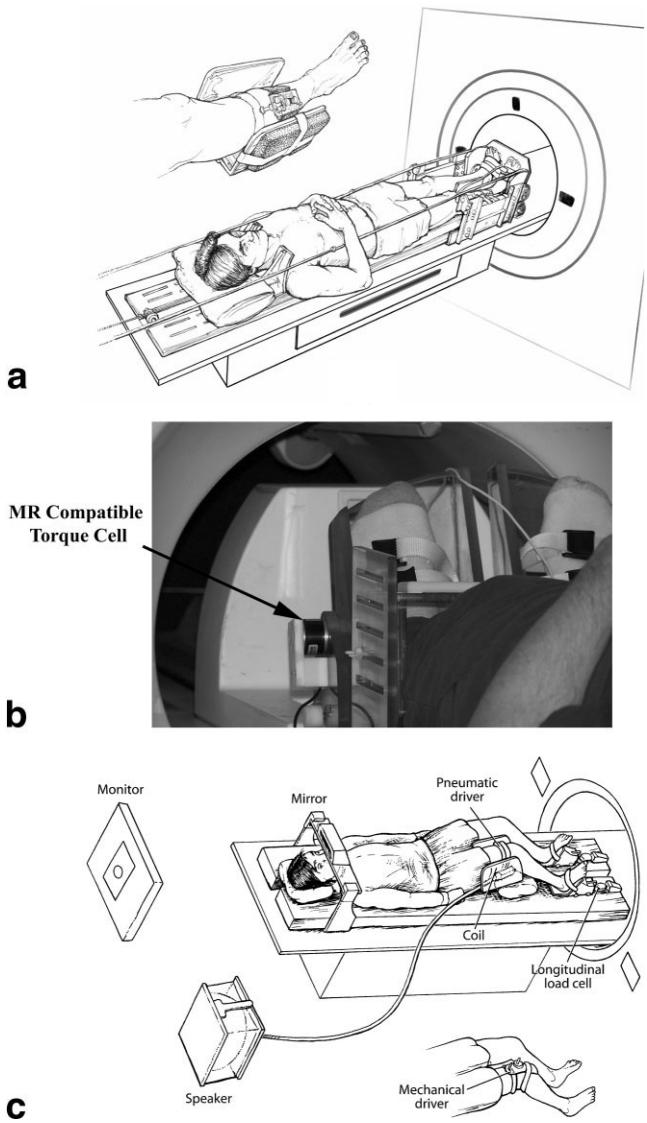

Figure 1. Examples of positioning and loading devices used to collect muscle MRE data. **a:** Weights connected to a cable and pulley system applied plantar flexion and dorsiflexion moments to the ankle joint. The ankle position could also be adjusted. Reprinted from Basford JR, Jenkyn TR, An K-N, Ehman RL, Heers G, Kaufman KR. Evaluation of healthy and diseased muscle with magnetic resonance elastography. Arch Phys Med Rehabil 2002;83:1530-1536, with permission of Elsevier (19,22,24). **b:** Photograph of a MR compatible torque cell incorporated into a positioning and loading device used to assess distal leg muscles. **c:** MR compatible leg press and examples of mechanical and pneumatic drivers used to induce shear waves into the proximal leg muscles. (Reprinted from Bensamoun SF, Ringleb SI, Littrell L, et al. Determination of thigh muscle stiffness using magnetic resonance elastography. J Magn Reson Imaging 2006;23:242-247, with permission of Wiley-Liss, Inc, a subsidiary of John Wiley & Sons, Inc.)

DATA PROCESSING

Numerous methods have been developed to invert MRE displacement data and to estimate the mechanical properties of the tissue (21,33–36). Most 2D and 3D inversion algorithms assume that tissue is linear, elastic, locally homogeneous, and isotropic. Because muscle is inhomogeneous and anisotropic, traditional inversion algorithms cannot be applied. However, with the assumption that the shear waves travel along the muscle fibers, the data can be analyzed along the local fiber direction. In initial studies a line profile was drawn along the local fiber direction in the MR magnitude image (Fig. 2a). This line profile was transferred to the displacement image (Fig. 2b) and the wave length (λ) (Fig. 2c) along the profile was measured. The wavelength was converted to wave speed (Eq. [2]), where f is the frequency of the induced vibrations. Finally, the shear stiffness (μ) was estimated (Eq. [3]), where the density of the tissue (ρ) was assumed to be 1000 kg/m^3 (23,27,30).

$$c = f\lambda \tag{2}$$

$$\mu = \rho c^2. \tag{3}$$

Other techniques have been implemented to analyze muscle MRE data. A Fourier transform was used to transform waveforms parallel to a line of propagation into the spatial frequency domain, and the spatial frequencies for each spectrum were averaged and inverted to calculate the wavelength (24). Equations [1] and [2] were then used to estimate the shear stiffness. Another method used to invert muscle data calculates the gradient of the phase of the wave along a profile aligned with the local fiber orientation. MRE data can be acquired at multiple phase offsets between the mechanical vibration and the oscillating magnetic gradients, which effectively captures the wave field at different times in the harmonic cycle. The phase gradient inversion method extracts the harmonic component of the shear wave at the driving frequency with a temporal

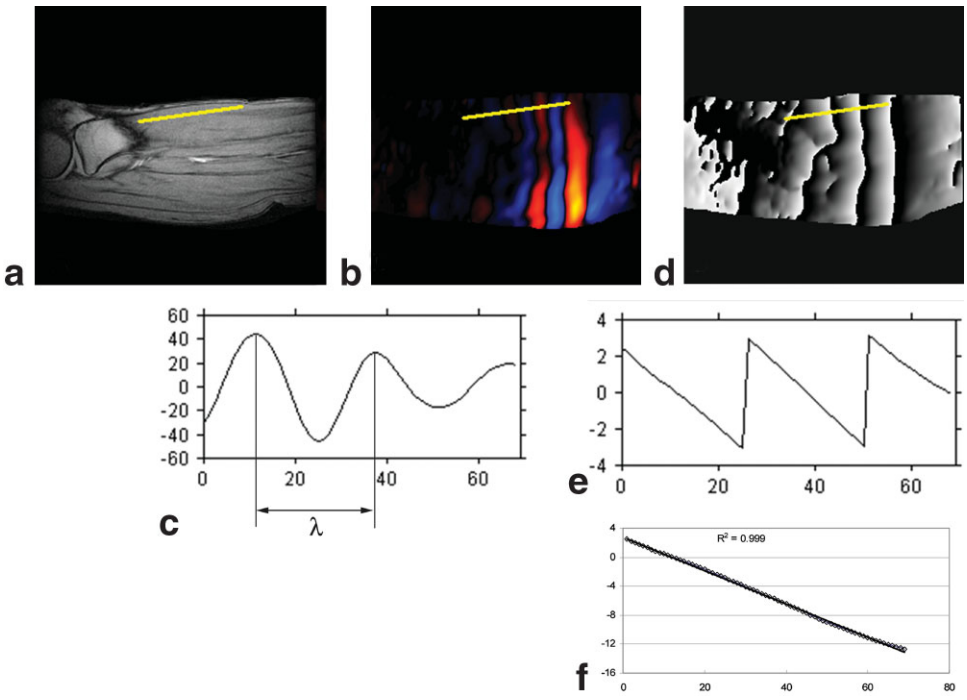

Figure 2. Example of data analysis in the tibialis anterior. **a:** A line profile was drawn along the local fiber direction of the tibialis anterior in the MR magnitude image and (**b**) copied to the displacement image. **c:** In one method of data analysis, the wavelength (λ) is measured from the line profile and the shear stiffness is estimated. In a second data analysis method, the line profile is copied from the magnitude image to the wave phase image (**d**), phase wraps (**e**,**f**) are removed, so that the slope can be calculated and the shear stiffness can be estimated.

Fourier transform, thus yielding the phase and amplitude of the propagating wave at each pixel (21). From these data, the gradient of the wave phase, which is inversely proportional to the local wavelength, can be used to calculate the stiffness. Specifically, a profile along the local fiber orientation is drawn as in Fig. 2a and transferred to the wave phase image (Fig. 2d), phase wraps (if present) are removed, and the slope of the line was calculated with a linear curve fitting algorithm (Fig. 2e and f). This slope, which equals the wave number (k), can then be converted to local wavelength (Eq. [4]), where field of view (FOV) is in meters and N is the number of pixels in the FOV. The shear stiffness can be calculated as above.

$$\lambda = \frac{FOV \cdot 2\pi}{k \cdot N}. \quad (4)$$

A coupled harmonic oscillator (CHO) simulation was developed to simulate 3D wave patterns in idealized anisotropic models of muscle using a set of ordinary coupled linear differential equations with varying coupling and damping coefficients to approximate the wave equation (Eq. [5]) (28), where u is the displacement, $\mathbf{W}$ is the coupling matrix, $\mathbf{F}$ is the position-dependent external driving force, Γ is the damping vector, and $\Gamma t >> 1$. The behavior of these patterns with different transverse and longitudinal coupling constants was studied and numerical values for the two shear stiffnesses determined from fits to 2D MRE observations under various model assumptions.

$$\frac{d^2}{dt^2}u(t) + \Gamma\frac{d}{dt}u(t) + Wu = F(t). \quad (5)$$

Alternatively, a 2D anisotropic waveform analysis was developed to determine anisotropic elastic coefficients in muscle (37). In this analysis, it is assumed that the principal axis of symmetry is parallel to the muscle fibers and the image plane is coincident with the stress plane, so that the stress is planar, thus reducing the governing equation for elastic wave propagation (Eq. [6]).

$$C_{11} = 4\mu_{12} = 2C_{13} \quad C_{33} = 4\mu_{12}E_3/E_1 \quad C_{55} = 2\mu_{13}. \quad (6)$$

A squared elliptic equation (Eq. [7]) was then used to develop an explicit relation between the waveform and the elasticity, which resulted in the shear stiffness (μ_{13}) and two Young's moduli (E_1 and E_3).

$$(e_1k_1^2 + 2e_2k_1k_3 + e_3k_3^2 + 2e_4k_1 + 2e_5k_3 + e_6)^2 = 0. \quad (7)$$

While this method has promise to improve our understanding of the results from muscle MRE, it may be difficult to satisfy the aforementioned assumptions and the requirement that boundary conditions are nonreflective in muscles with complex fiber orientations and/or morphology (e.g., the quadriceps).

A waveguide constrained method of analyzing MRE data was developed to analyze data from media in which the propagation of waves is constrained by wave guides, such as fiber bundles (38). After extracting the harmonic component at the driving frequency with a temporal Fourier transform as above, a Helmholtz decomposition was used to separate the displacement field into longitudinal and shear components, a spectral wave decomposition of the wave along the fibers was completed, and a sliding window Fourier transform was performed on the data resulting in space-wave number images (38–40). The maxima of these decompositions provided velocity profiles in the longitudinal

Table 1
Mean (SD) of the Shear Stiffness of Relaxed Muscles*

References	*N*	Upper extremity			Distal leg				Proximal leg		
		Biceps	FDP	Trap	TA	MG	LG	Sol	VL	VM	Sr
Dresner et al (23)	5	27.3 (11.9)	–	–	–	–	–	–	–	–	–
Basford et al (22)	8	–	–	–	12.0 (0.4)	24.9 (0.7)	16.2 (0.2)	16.8 (0.2)	–	–	–
Heers et al (19)[a]	6	–	–	–	11.9 (0.6)	20.3 (1.1)	16.4 (0.2)	16.4 (0.2)	–	–	–
Jenkyn et al (24)	1	–	–	–	12.3	–	22.0	–	–	–	–
Uffmann et al (27)	12	17.9 (5.5)	8.7 (2.8)	–	–	–	9.9 (6.8)	12.5 (7.3)	–	–	–
Bensamoun et al (30)	12–14	–	–	–	–	–	–	–	3.7 (0.9)	3.9 (1.2)	7.5 (1.6)
S.I. Ringleb (unpublished results)[a]	11	–	–	–	–	–	16.1 (2.2)	–	–	–	–
Q. Chen (unpublished results)	8	–	–	5.8 (2.0)	–	–	–	–	–	–	–

*Muscles tested in: 1) the upper extremity were the biceps brachii (biceps), flexor digitorum profundus (FDP), and trapezius (trap); 2) the distal leg were the tibialis anterior (TA), medial gastrocnemius (MG), lateral gastrocnemius (LG), and soleus (Sol); and 3) the proximal leg were the vastus lateralis (VL), vastus medialis (VM), and sartorius (Sr).
[a]Values are mean (standard error) from Heers et al (19) and S.I. Ringleb (unpublished results).

and transverse components. This technique was applied to multislice MRE data obtained from the tibialis anterior in a healthy volunteer. Wave speeds were evaluated along three fibers. The longitudinal component of the wave had a consistent velocity; however, the velocity and polarization of the transverse waves varied with the location of the wave (38). This technique is a promising method for understanding the mechanical properties of waves in 3D muscle data. However, the data acquisition time must be decreased before it can be clinically useful.

APPLICATIONS TO MUSCLE

MRE was successfully applied to healthy muscles in the biceps brachii (23,27,28,37), distal leg (e.g., tibialis anterior, gastrocnemius, and soleus) (19,24,26,27,32), flexor digitorum profundus (27), thigh muscles (30), and trapezius (Q. Chen, unpublished results). While some studies developed methods for collecting MRE data in specific muscles and reported a database of muscle stiffness under various testing conditions (24,27,30), other studies used MRE for specific tasks, such as validating a model of muscle behavior (23), correlating MRE to EMG (19), understanding how symmetric the shear stiffness of muscle is (26), and determining if significant changes in the shear stiffness occurred when pathology was present in the distal (22,26,31) and proximal (25) muscles of the leg.

DATABASES OF MUSCLE STIFFNESS USING MRE

The relaxed (Table 1) and contracted shear stiffness for muscles in the upper extremity, distal leg, and proximal leg were reported. The repeatability of muscle stiffness in the upper (27) and lower (32) extremities were reported. Methods were established to induce shear waves throughout a larger muscle (the upper trapezius) (Q. Chen, unpublished results) and to identify oblique scan planes that could be used to consistently visualize shear waves in the proximal thigh muscles (30). It was observed that changes in the wave shape and/or shear stiffness may be affected by muscle fiber type or morphology (30).

The repeatability of muscle MRE acquisition was assessed in the biceps brachii (27) and lateral gastrocnemius (32). Repeat data were collected in the relaxed biceps brachii of two volunteers over seven days. The mean and SD of the stiffness values of the repeat trials were calculated, and the SDs were 1.7 and 4.7 kPa for the two volunteers (27). Repeat data were collected from nine volunteers in the relaxed lateral gastrocnemius. The coefficient of variation was 15.7% and the mean SD was 2.32 kPa, which was comparable to the SDs reported in the biceps brachii. When the lateral gastrocnemius was contracted, the coefficient of variation was 19.4% and the SD increased to 5.2 kPa. These data were consistent with a repeat study of EMG data in the upper extremity over three years that found large variations at the individual level (41), suggesting that MRE measurements are as repeatable as the EMG activity in muscles.

The trapezius is frequently weakened or altered by primary injuries, such as overuse, or as a result of a regional disorder such as rotator cuff dysfunction, which can lead to debilitation of the muscles in the shoulder girdle. To use MRE to study these injuries, a large area of the upper trapezius must be investigated. Therefore, a study was completed to induce waves throughout the upper trapezius in a population of healthy volunteers ($N = 8$) (Q. Chen, unpublished results). With an oblique sagittal scan plane and the use of a carefully positioned pneumatic driver, planar waves were successfully induced in the area of interest (Fig. 3).

In the distal leg, the mean shear stiffness of the relaxed lateral gastrocnemius and the soleus (19,22) was smaller when these muscles were examined in the coronal plane (27). These data suggest that the differences in acquisition plane could significantly affect the stiff-

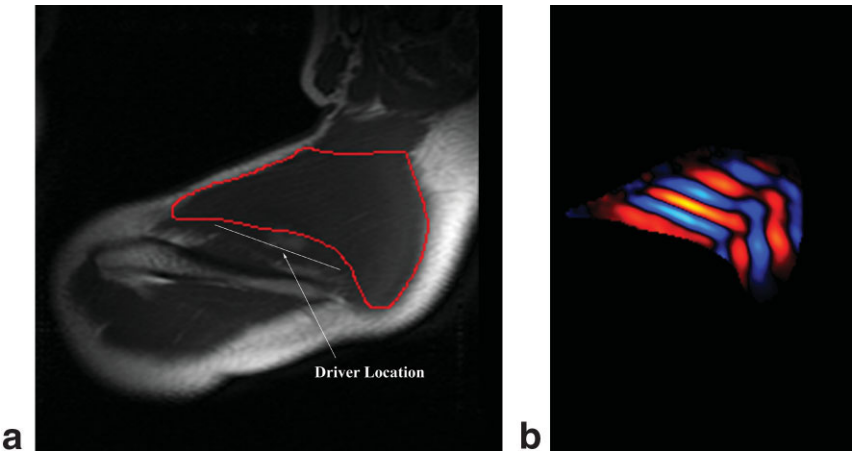

Figure 3. a: Magnitude image of the upper trapezius. The outlined region is the area of the muscle where planar wave fronts are desired. The location of the driver is indicated. **b:** Displacement image in the upper trapezius demonstrating that planar waves were successfully obtained in the region of interest.

ness estimate because muscle is not homogeneous or isotropic. Additionally, the propagation direction of the wave must also be contained within the acquisition plane or the stiffness estimates will be systematically biased. In the proximal leg muscles, the relaxed shear stiffness of the sartorius was significantly greater than the vastus muscles, indicating that muscle stiffness may be affected by orientation of the muscle fibers (i.e., the sartorius has longitudinal fibers, while the vastus muscles have pennate fibers). Qualitatively, the sartorius had round waves and the vastus muscles had elliptical waves (30). Additionally, it was noted that the oblique scan plane must be carefully selected in order to visualize propagating waves in these muscles (30).

An increase in shear stiffness was observed when the muscles were isometrically contracting (19,23,24). The proximal leg muscles were tested in a MR compatible leg press. When the volunteers extended their legs at 10% of the maximum voluntary contraction (MVC), there was a significant increase ($P < 0.05$) in the shear stiffness of the vastus lateralis and at 20% of the MVC, there was a significant increase in the shear stiffness of the vastus medialis. The shear stiffness in the vastus lateralis may have increased at a faster rate because it has more type II (fast) muscle fibers, while the vastus medialis has more type I (slow) muscle fibers. These findings suggest that MRE is capable of detecting differences in both muscle fiber orientation and muscle fiber type (30).

PREDICTION OF MUSCLE BEHAVIOR

A model was developed to predict the behavior of skeletal muscle using MRE (23). This model predicted that: 1) the shear stiffness of muscle would be positive with no loading and that passive tension will produce a linear shear stiffness increase where the slope is dependent on the cross-sectional area; and 2) shear stiffness will increase linearly with load when contracted isometrically and the slope of the shear stiffness vs. load curve would be related to the inverse of the volume and cross-sectional area of the muscle. This model was tested in vivo in the biceps brachii of five healthy, asymptomatic volunteers and with ex vivo bovine muscle. The first prediction was supported by in vivo data collected in the relaxed condition. The average shear stiffness in the biceps brachii was 27.3 kPa (range 8–34 kPa) (23), whereas the large variation in biceps stiffness was attributed to the differences in cross sectional area. In a subsequent study of the biceps brachii, a similar large range in biceps shear stiffness was observed (27). The ex vivo bovine muscle showed that the muscle's stiffness increased when it was stretched. Consistent with the second prediction, when the biceps were isometrically contracted, a linear increase in stiffness vs. applied load was observed, whereas the slope increased with a decrease in muscle size (23).

The first model prediction was examined and confirmed in the distal leg muscles. The lateral gastrocnemius and tibialis anterior were examined while the

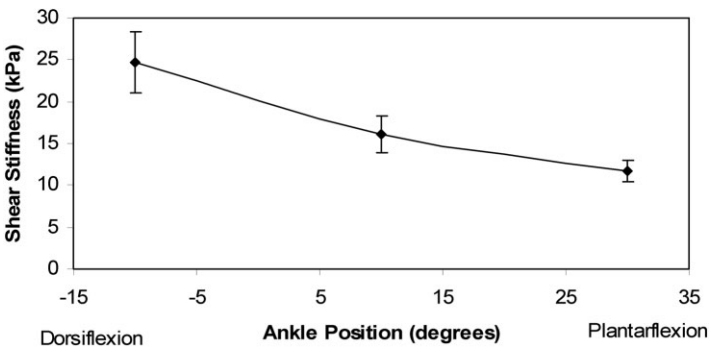

Figure 4. The mean ± standard error of the shear stiffness of the lateral gastrocnemius at different ankle positions indicates that the stiffness of the lateral gastrocnemius increases as the ankle moves toward dorsiflexion.

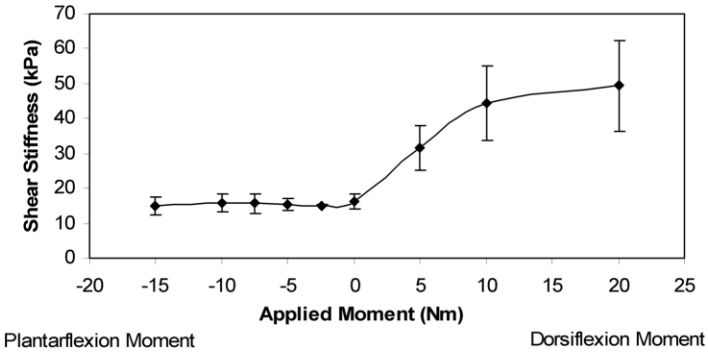

Figure 5. The mean ± standard error of the shear stiffness of the lateral gastrocnemius under isometric plantar flexion moments (i.e., the volunteer is dorsiflexing) and dorsiflexion moments (i.e., the volunteer is plantar flexing). The shear stiffness increased as the dorsiflexion moment increased, but there was no change in stiffness under a plantar flexion moment because the gastrocnemius is a plantar flexor.

muscles were relaxed at various ankle positions, thus changing the passive tension of the muscles. The shear stiffness was greatest when the ankle was dorsiflexed and decreased as the ankle was moved into plantar flexion (24) (Fig. 4). Conversely, the shear stiffness of the tibialis anterior was greatest when the ankle was plantar-flexed and was similar when the ankle was in neutral (0°) and in 20° of dorsiflexion (24).

The distal leg muscles were also examined while resisting plantar flexion and dorsiflexion moments (19,24) (Fig. 5). When a plantar flexion moment was applied (i.e., the volunteers were isometrically dorsiflexing), the shear stiffness of the tibialis anterior (a dorsiflexor) increased with load while there was no change in the shear stiffness of the gastrocnemius or soleus. Conversely, when the volunteers were isometrically plantar-flexing, the shear stiffness in the gastrocnemius and soleus increased significantly (19,24) and there was an insignificant increase in the shear stiffness of the tibialis anterior (19,24).

CORRELATION OF MRE DATA WITH A FUNCTIONAL EXAMINATION

It was hypothesized that the shear stiffness of distal leg muscles were correlated to muscle activity (19). The shear stiffness measured with MRE was compared to the EMG activity of the muscles under the same loading conditions. EMG data were collected with surface electrodes for the medial gastrocnemius, lateral gastrocnemius, and tibialis anterior, while fine wire EMG data were collected from the soleus. The R^2 values ranged from 0.82 to 0.90, suggesting a high linear correlation between the EMG and MRE measurements (19). The highest correlation was found in the soleus, suggesting that the correlations in the other three muscles may improve if a fine wire EMG electrode was used. This study demonstrated that MRE relates to an established measurement of assessing muscle activity. Additionally, some advantages of MRE were demonstrated including the fact that a large group of muscles can be examined simultaneously, the tension throughout a muscle can be investigated, MRE is noninvasive and MRE could be used to investigate the muscle properties while at rest (19).

ASSESSING PATHOLOGIC MUSCLE WITH MRE

Distal Leg Muscles

Toward the goal of using MRE to examine the muscles in pathologies that affect one side of the body (e.g., hemiplegia and disuse atrophy from a unilateral injury), a level of symmetry was established in the lateral gastrocnemius of 11 healthy, asymptomatic volunteers when the ankle was positioned passively, under plantar flexion loading and dorsiflexion loading. These data were used to determine a 95% confidence interval (CI), that when exceeded will indicate when differences in the shear stiffness of muscle are due to normal anatomic variations or the pathology (32). In the lateral gastrocnemius, the upper and lower limits of an asymmetry threshold (A_{UL}) were ± 8.7% when the muscle was relaxed and ±11.6% when an isometric plantar flexion load was applied. These limits of asymmetry were exceeded by 11 patients with hemiparesis as a result of stroke (32).

Two additional studies have found that MRE is capable of detecting differences between healthy and pathologic muscle in the lower limb. The shear stiffness of the lateral gastrocnemius, medial gastrocnemius, soleus, and tibialis anterior in patients with poliomyelitis (N = 1), flaccid paraplegia (N = 2), and spastic paraplegia (N = 3) were compared to a database of healthy volunteers (N = 8). Data were collected when the muscles were relaxed and the ankles were in the neutral position. Significant increases in shear stiffness were measured in all four muscles (22). In a subsequent study, the shear stiffness of the soleus in men with hypogonadism was compared to healthy volunteers with the ankle fixed at 90° when the muscles were relaxed and from 5% to 20% of the maximum voluntary contraction. There was no significant difference between the absolute shear stiffness, however, when normalized to the resting shear stiffness, a significant difference ($P < 0.05$) was found between the healthy and pathologic muscles (31).

Proximal Leg Muscles

Several diseases such as hyperthyroidism cause proximal muscle weakness, which may result in a change in the shear stiffness. In Graves disease (hyperthyroidism), there is a decrease in the number of slow-twitch muscle fibers and an increase in fast-twitch muscle

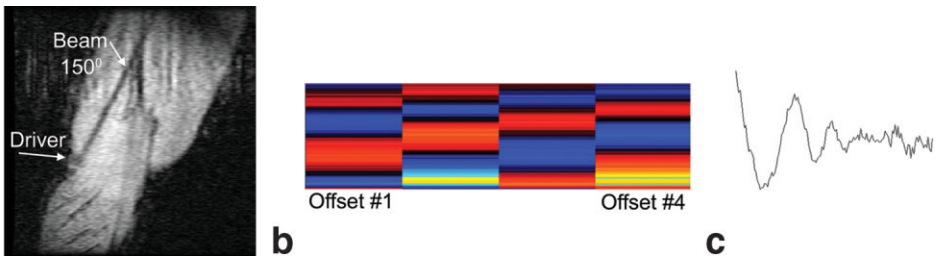

Figure 6. Example of 1D MRE. The location of the 1D profile (beam) in the vastus medialis (**a**), the 1D wave displacement image (**b**), and the profile of the wave in 1D (**c**).

fibers (42). The relationship between the shear stiffness and applied load in the vastus medialis in healthy volunteers ($N = 5$) and patients with Graves disease ($N = 5$) was investigated. This study found that patients with Graves disease had a faster increase in muscle stiffness after treatment than healthy volunteers (25), due to a period of repair and adaptation of the thigh muscle fibers. While a larger sample size is needed, MRE may be capable of noninvasively detecting transformations in muscle fiber type.

ONE-DIMENSIONAL MRE

A 1D MRE acquisition technique (43) was used to evaluate the shear stiffness of the vastus medialis and compared with the aforementioned 2D technique (44) (Fig. 6). The mean stiffness of the vastus medialis measured at rest was 3.7 and 4.4 kPa using the 1D and 2D techniques, respectively. At 20% of the maximum voluntary contraction, the stiffness increased to 9.5 and 9.22 kPa in the 1D and 2D techniques, respectively. This study determined that the 1D technique yields results equivalent to the 2D MRE technique, while decreasing the scan time by a factor of 4.5.

FUTURE DIRECTIONS

MRE has been successfully implemented in evaluating several major muscle groups in the upper extremities (i.e., trapezius, biceps brachii, and flexor digitorum profundus), the thigh muscles (i.e., vastus lateralis, vastus medialis, and sartorius), and the distal leg (i.e., tibialis anterior, soleus, medial gastrocnemius, and lateral gastrocnemius). Because muscle is inhomogeneous and anisotropic, efforts toward developing inversions that can consider anisotropy in muscles with complex morphologies and fiber structures in three dimensions should continue. Finite element modeling of muscle, including its anisotropic properties, may also improve our understanding of the behavior of shear waves in skeletal muscle. Additionally, faster pulse sequences must be investigated, such as echo planar imaging (EPI) sequences, to decrease the acquisition time, such that 3D data can be obtained when muscles are contracted. 1D MRE acquisitions can also be examined in different muscles and can be investigated as a method to monitor real time changes during active contractions.

It will be helpful to determine how MRE correlates to commonly used clinical measures, such as muscle biopsy and subjective scales commonly used to evaluate pathologies. If muscle MRE is compared to muscle biopsies in either human or animal studies, we can determine if it is possible to use MRE to detect changes in fiber type. The modified Ashworth scale is commonly used to measure the amount of spasticity in patients. Correlating this scale with muscle MRE will give clinicians a quantitative measure of spasticity, which may help evaluate treatment methods.

MRE was shown to detect differences between healthy and pathologic muscles in the lower extremities (22,25,26,31); therefore, it is practical to start using MRE to answer specific clinical questions in pathologies that effect muscles. For example, MRE can be used to evaluate treatments for muscles altered by pathology (e.g., hyperthyroidism and stroke) and injured muscle (e.g., muscle atrophy caused by disuse). The evaluation of treatment methods that typically use subjective measures to evaluate their effectiveness may improve treatment drastically because it can be used to determine what method is most effective. Additionally, MRE can be used to understand pathologies that present similarly, but have different functional outcomes, such as ankle ligament damage, in which some patients have functionally unstable ankles while others function normally.

ACKNOWLEDGMENT

We thank Krista A. Coleman-Wood, PhD, PT, for her assistance.

REFERENCES

1. Bizzini M, Mannion AF. Reliability of a new, hand-held device for assessing skeletal muscle stiffness. Clin Biomech 2003;18:459–461.
2. Leonard CT, Brown JS, Price TR, Queen SA, Mikhailenok EL. Comparison of surface electromyography and myotonometric measurements during voluntary isometric contractions. J Electromyogr Kinesiol 2004;14:709–714.
3. Arokoski JP, Surakka J, Ojala T, Kolari P, Jurvelin JS. Feasibility of the use of a novel soft tissue stiffness meter. Physiol Meas 2005; 26:215–228.
4. Leonard CT, Deshner WP, Romo JW, Suoja ES, Fehrer SC, Mikhailenok EL. Myotonometer intra- and interrater reliabilities. Arch Phys Med Rehabil 2003;84:928–932.
5. Sinha S, Hodgson JA, Finni T, Lai AM, Grinstead J, Edgerton VR. Muscle kinematics during isometric contraction: development of phase contrast and spin tag techniques to study healthy and atrophied muscles. J Magn Reson Imaging 2004;20:1008–1019.
6. Finni T, Hodgson JA, Lai AM, Edgerton VR, Sinha S. Mapping of movement in the isometrically contracting human soleus muscle reveals details of its structural and functional complexity. J Appl Physiol 2003;95:2128–2133.
7. Finni T, Hodgson JA, Lai AM, Edgerton VR, Sinha S. Nonuniform strain of human soleus aponeurosis-tendon complex during submaximal voluntary contractions in vivo. J Appl Physiol 2003;95: 829–837.

8. Finni T, Hodgson JA, Lai AM, Edgerton VR, Sinha S. Muscle synergism during isometric plantar flexion in Achilles tendon rupture patients and in normal subjects revealed by velocity-encoded cine phase-contrast MRI. Clin Biomech (Bristol, Avon) 2006;21:67–74.
9. Zhong X, Blemker SS, Spottiswoode BS, Helm PA, Hess AT, Epstein FH. Application of cine DENSE MRI to studying skeletal muscle mechanics during joint motion. In: Proceedings of the 14th Annual Meeting of ISMRM, Seattle, WA, USA, 2006 (Abstract 256).
10. Adams GR, Duvoisin MR, Dudley GA. Magnetic resonance imaging and electromyography as indexes of muscle function. J Appl Physiol 1992;73:1578–1583.
11. Ploutz LL, Tesch PA, Biro RL, Dudley GA. Effect of resistance training on muscle use during exercise. J Appl Physiol 1994;76:1675–1681.
12. Yue G, Alexander AL, Laidlaw DH, Gmitro AF, Unger EC, Enoka RM. Sensitivity of muscle proton spin-spin relaxation time as an index of muscle activation. J Appl Physiol 1994;77:84–92.
13. Gold GE. Dynamic and functional imaging of the musculoskeletal system. Semin Musculoskelet Radiol 2003;7:245–248.
14. Meyer RA, Towse TF, Reid RW, Jayaraman RC, Wiseman RW, McCully KK. Bold MRI mapping of transient hyperemia in skeletal muscle after single contractions. NMR Biomed 2004;17:392–398.
15. Levinson SF, Shinagawa M, Sato T. Sonoelastic determination of human skeletal muscle elasticity. J Biomech 1995;28:1145–1154.
16. Gennisson JL, Catheline S, Chaffai S, Fink M. Transient elastography in anisotropic medium: application to the measurement of slow and fast shear wave speeds in muscles. J Acoust Soc Am 2003;114:536–541.
17. Levinson SF, Catheline S, Fink M. Anisotropic elasticity and viscosity deduced from supersonic shear imaging in muscle. International Society of Biomechanics, XXth Congress. 29th Annual Meeting of the American Society of Biomechanics, Cleveland, OH. p 101.
18. Gennisson JL, Cornu C, Catheline S, Fink M, Portero P. Human muscle hardness assessment during incremental isometric contraction using transient elastography. J Biomech 2005;38:1543–1550.
19. Heers G, Jenkyn T, Alex Dresner M, et al. Measurement of muscle activity with magnetic resonance elastography. Clin Biomech (Bristol, Avon) 2003;18:537–542.
20. Muthupillai R, Lomas D, Rossman P, Greenleaf JF, Manduca A, Ehman RL. Magnetic resonance elastography by direct visualization of propagating acoustic strain waves. Science 1995;269:1854–1857.
21. Manduca A, Oliphant TE, Dresner MA, et al. Magnetic resonance elastography: Non-invasive mapping of tissue elasticity. Med Image Anal 2001;5:237–254.
22. Basford JR, Jenkyn TR, An K-N, Ehman RL, Heers G, Kaufman KR. Evaluation of healthy and diseased muscle with magnetic resonance elastography. Arch Phys Med Rehabil 2002;83:1530–1536.
23. Dresner M, Rose G, Rossman P, Muthupillai R, Manduca A, Ehman RL. Magnetic resonance elastography of skeletal muscle. J Magn Reson Imaging 2001;13:269–276.
24. Jenkyn TR, Ehman RL, An KN. Noninvasive muscle tension measurement using the novel technique of magnetic resonance elastography (MRE). J Biomech 2003;36:1917–1921.
25. Ringleb SI, Littrell L, Chen Q, et al. Magnetic resonance elastography for the assessment of muscles in hyperthyroidism. In: 28th Annual Meeting of the American Society of Biomechanics, 2004; Portland, OR.
26. Ringleb SI, Kaufman KR, Basford JR, Ehman RL, An KN. Bilateral symmetry of the gastrocnemius stiffness measured with magnetic resonance elastography in healthy and pathologic muscle. International Society of Biomechanics, XXth Congress, 29th Annual Meeting of the American Society of Biomechanics, 2005; Cleveland, OH. p 373.
27. Uffmann K, Maderwald S, Ajaj W, et al. In vivo elasticity measurements of extremity skeletal muscle with MR elastography. NMR Biomed 2004;17:181–190.
28. Sack I, Bernarding J, Braun J. Analysis of wave patterns in MR elastography of skeletal muscle using coupled harmonic oscillator simulations. Magn Reson Imaging 2002;20:95–104.
29. Chan QCC, Li G, Ehman RL, Yang ES. Observation of anisotropic properties of skeletal muscle in MR elastography via a needle device. In: Proceedings of the 14th Annual Meeting of ISMRM, Seattle, WA, USA, 2006 (Abstract 1704).
30. Bensamoun SF, Ringleb SI, Littrell L, et al. Determination of thigh muscle stiffness using magnetic resonance elastography. J Magn Reson Imaging 2006;23:242–247.
31. Galban CJ, Maderwald S, Herrmann BL, et al. Measuring skeletal muscle elasticity in patients with hypogonadism by MR elastography. In: Proceedings of the 13th Annual Meeting of ISMRM, Miami Beach, FL, USA, 2005 (Abstract 2016).
32. Ringleb SI, Kaufman KR, Basford JR, et al. Magnetic resonance elastography: A non-invasive method to differentiate between healthy and pathologic muscle stiffness. 30th Annual Meeting of the American Society of Biomechanics, 2006, Blacksburg, VA.
33. Sinkus R, Lorenzen J, Schrader D, Lorenzen M, Dargatz M, Holz D. High-resolution tensor MR elastography for breast tumour detection. Phys Med Biol 2000;45:1649–1664.
34. Van Houten E, Miga M, Weaver J, Kennedy F. Three-dimensional subzone-based reconstruction algorithm for MR elastography. Magn Reson Med 2001;45:827–837.
35. Romano A, Shirron J, Bucaro J. On the noninvasive determination of material parameters from a knowledge of elastic displacements: theory and numerical simulation. IEEE Trans Ultrason Ferroelectr Freq Control 1998;45:751–759.
36. Romano A, Bucaro J, Ehman R, Shirron J. Evaluation of a material parameter extraction algorithm using MRI based displacement measurements. IEEE Trans Ultrason Ferroelectr Freq Control 2000;47:1575–1581.
37. Papazoglou S, Braun J, Hamhaber U, Sack I. Two-dimensional waveform analysis in MR elastography of skeletal muscles. Phys Med Biol 2005:1313–1325.
38. Romano AJ, Abraham PB, Ringleb SI, Rossman PJ, Bucaro JA, Ehman RL. Analysis of anisotropic velocity profiles utilizing waveguide constrained magnetic resonance elastography. In: Proceedings of the 14th Annual Meeting of ISMRM, Seattle, WA, USA, 2006 (Abstract 1725).
39. Romano AJ, Abraham PB, Ringleb SI, Rossman PJ, Bucaro JA, Ehman RL. Analysis of anisotropic propagation utilizing waveguide constrained magnetic resonance elastography. In: Proceedings of the 13th Annual Meeting of ISMRM, 2005; Miami Beach, FL, USA (Abstract 2556).
40. Romano AJ, Abraham PB, Rossman PJ, Bucaro JA, Ehman RL. Determination and analysis of guided wave propagation using magnetic resonance elastography. Magn Reson Med 2005;54:893–900.
41. Roe C, Steingrimsdottir OA, Knardahl S, Bakke ES, Vollestad NK. Long-term repeatability of force, endurance time and muscle activity during isometric contractions. J Electromyogr Kinesiol 2006;16:103–113.
42. Canepari M, Cappelli V, Pellegrino MA, Zanardi MC, Reggiani C. Thyroid hormone regulation of MHC isoform composition and myofibrillar ATPase activity in rat skeletal muscles. Arch Physiol Biochem 1998;106:308–315.
43. Glaser KJ, Felmlee JP, Ehman RL. Rapid shear stiffness estimations using 2-D spatial excitations in magnetic resonance elastography. In: Proceedings of the 10th Annual Meeting of ISMRM, Honolulu, HI, USA, 2002 (Abstract 39).
44. Bensamoun SF, Glaser K, Chen Q, Ringleb SI, Ehman RL, An KN. Rapid magnetic resonance elastography of skeletal muscle using one dimensional projection. 5th World Congress of Biomechanics, 2006. p 4631.